LAVA FLOW SUSCEPTIBILITY MAP OF MT ETNA BASED ON NUMERICAL SIMULATIONS

Annalisa Cappello
Ist. Naz. Geofisica e Vucanologia
Sezione di Catania
Italy
cappello@ct.ingv.it

Ciro Del Negro
Ist. Naz. Geofisica e Vucanologia
Sezione di Catania
Italy
delnegro@ct.ingv.it

Annamaria Vicari
Ist. Naz. Geofisica e Vucanologia
Sezione di Catania
Italy
vicari@ct.ingv.it

Abstract

We constructed maps of probability of lava inundation using computer simulations considering the past eruptive behaviour of the Mt. Etna volcano and data deriving from monitoring networks.

The basic a priori assumption is that new volcanoes will not form far from existing ones and that such a distribution can be performed using a Cauchy kernel. Geophysical data are useful to update or fine tune the initial Cauchy kernel to better reflect the distribution of future volcanism. In order to obtain a final susceptibility map, a statistical analysis permits a classification of Etna's flank eruptions into twelve types.

The simulation method consists of creating a probability surface of the location of future eruption vents and segmenting the region according to the most likely historical eruption on which to base the simulation.

The paths of lava flows were calculated using the MAGFLOW Cellular Automata (CA) model, allowing us to simulate the discharge rate dependent spread of lava as a function of time.

Key words

volcanic hazard, Cellular Automata model, lava flow

1 Introduction

Mt Etna will undoubtedly erupt again. When it does, the first critical question that must be answered is: Which areas are threatened with inundation? Once the threatened areas are established, we can address the second critical question: What people, property, and facilities are at risk? These questions can be answered by estimating the areas most likely to be affected by eruptions on various parts of the volcano.

Knowledge of the likely path and rate of advance of the front of a lava flow is of potential value for organizing both evacuations and mitigation efforts during the period of flow. Knowledge of the probability of a particular site being overrun by a lava flow is useful for long-term planning purposes.

The aim of this work is to compute hazard maps that can be used as a general guide to assist emergency managers during an eruption, to plan emergency response activities, and to identify communities and infrastructure at risk.

2 Methodology

We have defined a methodology for the compilation of a new kind of map showing the hazard related to lava invasion in predefined study areas.

A hazard map provides the probability that given areas will be affected by potential destructive volcanic processes. Its evaluation is generally based on the past eruptive behaviour of volcanoes and on data obtained by the monitoring networks.

In order to compute hazard maps, the following steps should be computed:

a) Definition of the source area;
b) Computation of susceptibility map (that provides the spatial probability of vent opening);
c) Characterization of the expected eruptions;
d) Evaluation of the temporal probability for the occurrence of the hazard during the considered time interval;
e) Numerical simulations of eruptive process and
f) Construction of the hazard map.

Mt Etna (Sicily, Italy) was chosen as the study area since it as one of the most dangerous in terms of possible fracture reactivation.

Having defined the study area, we have developed a methodology for estimating the long-term future spatial and temporal patterns in the Mt Etna. First a mid/long-term susceptibility map is generated, and then geophysical data are incorporated to develop the final susceptibility map.

For the aim of this study, we took advantage of a database containing the main volcanological data of all eruptions at Mt Etna since 1600. Mid/long-term susceptibility maps of Etna have been generated using the

following data: location of vents, fractures and vent alignments.

All available datasets have been converted into a probability density function (PDF). Each of the PDFs should be given a relevance value (which measures its importance) and a reliability value (which measures the quality of the dataset) with respect to the evaluation of the susceptibility. Finally, the PDFs and their relative values are combined through a Poisson process.

In the first stage a local intensity function λ_{xy} is computed using the kernel technique. A kernel function is a density function used to obtain the intensity of volcanic events at a sampling point x_p, y_p, calculated as a function of the distance to nearby volcanoes and a smoothing constant *h*. In estimating local volcanic densities in volcanic fields, the kernel function used is the Cauchy kernel.

For the two-dimensional Cauchy kernel, the calculation of λ_{xy} at the grid point x_p, y_p is

$$\lambda_{xy} = \frac{1}{\pi h^2 N} \sum_{i=1}^{N} \left\{ \frac{l_i}{1 + \left(\frac{d_i}{h}\right)^2} \right\} \qquad (1)$$

where d_i is the distance between x_p, y_p and the ith volcanic event, N is the number of volcanic events considered in the calculation and l_i is a factor for weighting eruption volume of the corresponding ith volcanic event.

Figure 1 shows an example of PDF generated considering only past vent locations, a 1 km grid spacing and a smoothing coefficient of 2 km.

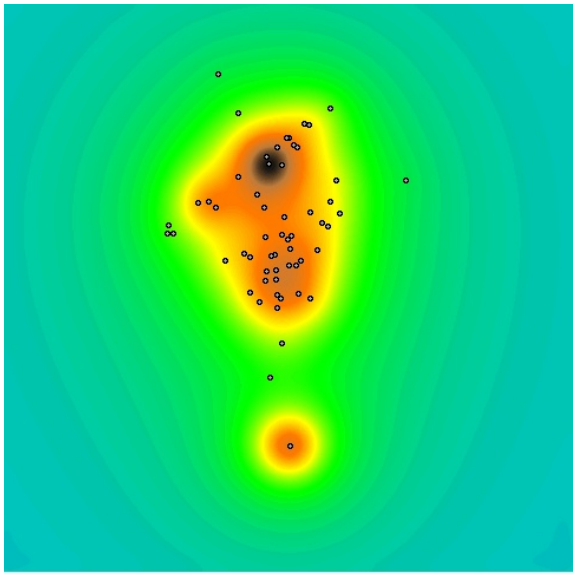

Figure 1. An example of PDF based on past vent locations

Probability estimates for each grid point x_p, y_p are computed by using a Poisson distribution where λ_{xy} represents the intensity function normalized to unity across the entire area:

$$P_{xy}\{N(t) \geq 1\} = 1 - exp(-t\lambda_t\lambda_{xy}\Delta x\Delta y) \qquad (2)$$

where $N(t)$ represents the number of future volcanic events that occur within time t and area $\Delta x\Delta y$.

Having generated the PDF based on past, the next step is to condition it with additional data deriving from geophysical data. This step represents the short-term analysis performed using data provided by the monitoring networks. The corresponding PDF should be evaluated using the same procedure.

Once all the PDFs has been calculated, they are combined (with an assigned relevance) in order to obtain the final susceptibility map.

For the characterization of the volcanic events we based on the knowledge of past eruptions to fix four different volumes of total fluxes: 6, 20, 50 and 200 m^3.

Then we established short, medium and large times of eruptions, setting respectively 15, 30 and 60 days of simulation.

Combining these values with random distribution, we obtained twelve possible functions representing the variation of flux rate in relation to the time of eruption.

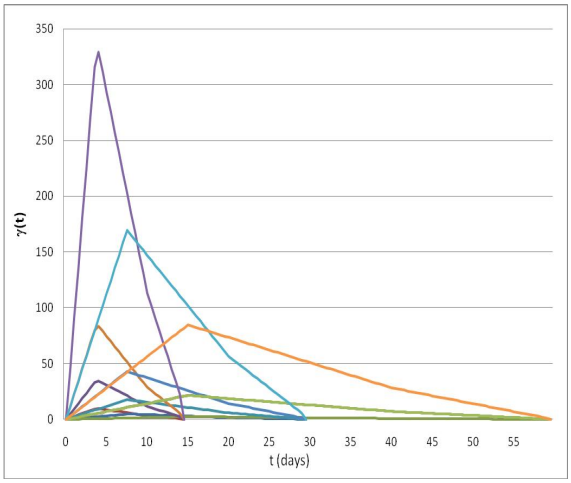

Figure 2. Values of flux rate-days of eruption used for the simulations.

The shape of the curves has been considered as a kind of bell, in which the eruption starts from a low value of flux rate, reaching its maximum value after a 1/4 of the entire time of simulation. After 2/3 of the maximum time of simulation reaches 1/3 of the maximum value and, finally, gradually decrease until the end of the eruption is reached (Figure 2).

The susceptibility map assigns a probability of activation to each vent in the grid. Next step is the calculation

of maps that assign a probability to each type of considered effusion rate and duration (event probability), devised on the basis of the emission behavior analysis of the study area.

For every type i of eruption, the positional data y_i are been used to estimate the type i intensity function $\lambda_i(x)$ for each point x of the grid using the kernel estimator described by [Diggle, 1900].

When j is an index of events in a category, i is a type of category, n is the total number of events in a category, then

$$\lambda_i(x; h_i) = h_i^{-2} \sum_{j=1}^{n_i} G\left\{\frac{x - y_{ij}}{h_i}\right\} \qquad (3)$$

where h_i is a smoothing parameter that controls the size of the zone to which each data point contributes an increased intensity, and G is the truncated normal kernel

$$G(x) = \begin{cases} 0.5\pi e^{-0.5x'x} & x'x < 1 \\ 0 & x'x > 1 \end{cases} \qquad (4)$$

The intensity function $\lambda_i(x)$ is then rescaled through the entire area.

The choice of the parameter h_i is determinant for the calculation of the estimator. Its value for each type of event is chosen using the existing data. First of all, it is necessary to examine the strength of spatial autocorrelation in the data at different scales. This is tested using the adjusted semi-variogram

$$2\bar{\gamma}(h) = \frac{\left\{\frac{1}{|N(h)|}\sum_{N(h)}\sqrt{|z(P_i) - z(P_j)|}\right\}^4}{\left(0.457 + \frac{0.494}{|N(h)|}\right)} \qquad (5)$$

where $z(P_i)$ is the observed value at the point P_i, h is a specified distance, and $N(h)$ is the set of pairs separated by a distance near to h.

For each data set in turn, the set of pairs of points is divided into suitable equal sized subsets. Each subset is used to calculate the statistic.

The semi-variogram grows with increasing h until it reaches a constant level. The h-value at which it reaches this sill correspond to the distance at which autocorrelation disappears.

Once the activation and the event probabilities are developed, numerical simulations could be computed. We used the MAGFLOW model for lava flow simulations based on Cellular Automatons [Del Negro et al., 2006; Vicari et al., 2007].

The simulations were performed using the typical parameters of Etnean lava flows. A grid of vents is defined in the study area, and a prefixed number of simulations is executed for each of them, each one characterized by its own effusion rate and duration.

Finally, the resulting hazard map is thus compiled by taking into account both information on lava flows overlapping, and their occurrence probability. This map is obtained by evaluating the hazard at each point in the study area as follows:

1. for each simulation, the hazard related to a generic point in the study area is computed as the product of the defined probabilities of occurrence (conditioned probability) if it is affected by the simulated lava flow, zero otherwise;
2. for each point, the conditioned probabilities are added over all the performed simulations.

The accuracy of the results strictly depends on the reliability of the simulation model, on the quality of input data and on the hypotheses on assigning the different probabilities of occurrence.

3 Conclusion

This work represents a preliminary methodology of applying computer simulation techniques to the assessment of hazard from lava flows. Using this method, MAGFLOW can be used to provide a series of simulation of lava flows and to produce most probable eruption scenarios.

Any number of simulations can be created by sampling the probability surface and parameter of simulator. Much improvement can be done, as for example separation of different type of eruptions, or a better specification of probability surface of the location of future vents.

Another improvement can be the introduction of a screening distance value (SDV) corresponding to the maximum distance from the source to the site at which the phenomenon could be a hazard. SDvs offer a way of arriving at realistic assessment of hazards based on a conservative worst-case scenario for the potential impact of each type of hazard.

References

Coltelli, M., Proietti, C., Branca, S., Marsella, M., Andronico, D., Lodato, L., (2007). *Analysis of the 2001 lava flow eruption of Mt. Etna from 3D mapping*, JGR 112, F02029, doi:10.1029/2006JF000598.

Crisci, G.M., Iovine, G., Di Gregorio, S., Lupiano, V., (2008). *Lava-flow hazard on the SE flank of Mt. Etna (Southern Italy)*. Journal of Volcanology and Geothermal Research 177, 778-796.

Del Negro , C., Fortuna, L., Herault, A., Vicari, A., (2006). *Simulations of the 2004 lava flow at Etna volcano by the magflow cellular automata model*, Bull. Volcanol., doi:10.1007/s00445-007-0168-8.

Diggle, P.J., (1900). *A point process modelling approach to raised incidence of a rare phenomenon in the vicinity of a prespecified point*, J. R. Stat. Soc., Ser. A, 153, 349-362.

Felpeto, A., Marti, J., Ortiz, R., (2007). *Automatic GIS-based system for volcanic hazard assessment*. Journal of Volcanology and Geothermal Research 166, 106-116.

Martin, A.J., Umeda, K., Connor, C.B., Weller, J.N. Zhao, D., Takahashi, M., (2004). *Modeling long-term volcanic hazards through Bayesian inference: an example from the Tohuku volcanic arc, Japan*. JGR 109, B10208.

McBirney, A. R., Serva, L., Guerra, M., Connor, C. B., (2003). *Volcanic and seismic hazards at a proposed nuclear power site in central Java*. Journal of Volcanology and Geothermal Research 126, 11-30.

Vicari, A., Herault, A., Del Negro, C., Coltelli, M., Marsella, M., Proietti, C., (2007). *Modeling of the 2001 lava flow at Etna volcano by a cellular automata approach*. Environmental Modelling & Software 22, 1465-1471

Wadge, G., Young, P.A.V., McKendrick, I.J., (1994). *Mapping lava flow hazards using computer simulation*. JGR 99 (B1), 489-504.